Human Organotypic Retinal Cultures (HORCs) as a Chronic Experimental Model for investigation of Retinal Ganglion Cell Degeneration

Andrew Osborne[a, b], Marina Hopes[a, c], Phillip Wright[a], David C Broadway[a, c, d], Julie Sanderson[a]*

[a]School of Pharmacy, University of East Anglia, Norwich, NR4 7TJ, UK

[b]John van Geest Centre for Brain Repair, University of Cambridge, Cambridge, CB2 0PY, UK

[c]Department of Ophthalmology, Norfolk and Norwich University Hospital, Norwich, NR4 7UY, UK

[d]School of Biological Sciences, University of East Anglia, Norwich, NR4 7TJ, UK

*corresponding author: j.sanderson@uea.ac.uk

Abstract

There is a growing need for models of human diseases that utilise native, donated human tissue in order to model disease processes and develop novel therapeutic strategies. In this paper we assessed the suitability of aged human retinal explants as a potential model of chronic retinal ganglion cell (RGC) degeneration. Our results confirmed that RGC markers commonly used in rodent studies (NeuN, βIII Tubulin and Thy-1) were appropriate for labelling human RGCs and followed the expected differential expression patterns across, as well as throughout, the macular and para-macular regions of the retina. Furthermore, we showed that neither donor age nor *post-mortem* time (within 24 hours) significantly affected the initial expression levels of RGC markers. In addition, the feasibility of using human *post mortem* donor tissue as a long-term model of RGC degeneration was determined with RGC protein being detectable up to 4 weeks in culture with an associated decline in RGC mRNA and significant, progressive, apoptotic labelling of $NeuN^+$ cells. Differences in RGC apoptosis might have been influenced by medium compositions indicating that media constituents could play a role in supporting axotomised RGCs. We propose that using *ex vivo* human explants may prove to be a useful model for testing the effectiveness of neuroprotective strategies.

Keywords: human, RGC, glaucoma, model, retina, apoptosis, degeneration

Abbreviations: HORCs – human organotypic retinal cultures

RGCs – retinal ganglion cells

1 Introduction

Organotypic retinal cultures provide an important link between dissociated cell cultures and *in vivo* models (Johnson et al., 2011), benefiting from maintenance of heterogeneous cell populations that can be observed *in situ* (Caffé et al., 2001). Although cultures of dissociated cells are helpful in elucidating the direct effect of drugs on individual cell types, the loss of intercellular relationships limits their usefulness when modelling complex diseases (Buyens et al., 2014). At the other end of the spectrum, animal models that more closely resemble actual pathologies are costly, time consuming and the outcomes can be difficult to correlate with human conditions. Furthermore, there is a recognized demand for *in vitro* models that can replace or reduce the need for animal experiments.

Although research using retinal explants has increased over recent years, the use of human retinal explants is still underutilised. Research using rodent retinal organotypic cultures is now common but it is recognised that differences exist between rodent and human retina (Albrecht May, 2008; Bobu et al., 2008; Levkovitch-Verbin, 2004). The most significant difference between mouse and human retina is that the human retina has a central macula and fovea for high-resolution colour vision, in addition to different ratios of cone and rod photoreceptors with specific topography and subtypes of retinal ganglion cells (RGCs). Using human retina therefore, provides the most appropriate tissue to model a variety of human eye diseases.

Some of the factors limiting the advancement of human retinal models are that questions remain to be answered regarding donor variability, the effects of *post mortem* time and the potential time scale that the human retina can survive in culture.

There are also practical issues to consider, such as whether markers used in animal experiments are appropriate for use in human research. The present paper aimed to investigate these questions.

Firstly, the expression and labelling of numerous RGC markers was investigated across the human retina within the macular and para-macular regions. In addition, the variation of RGC mRNA expression was evaluated from numerous *post mortem* donor eyes to address concerns relating to donor variability. Further work to address possible effects of *post mortem* time on tissue viability were assessed through the comparison of retina derived immediately after orbital exenteration from living donors and those from eyes obtained at varying times after donor patient death. Secondly, we aimed to assess the feasibility of using adult human retina in a long-term culture system for studying RGC degeneration. We have previously shown that adult human organotypic retinal cultures (HORCs) can be used to investigate RGC death following brief ischaemic injury (Niyadurupola et al., 2013; Osborne et al., 2015) and glutamate excitotoxicity (Niyadurupola et al., 2011), but degeneration over time points longer than 48 hours had not been investigated. Human embryonic (Engelsberg et al., 2008) and foetal (Donovan and Dyer, 2006; Rojas et al., 2003; Zhang et al., 2010) retinal explants have been cultured for up to 42 days with preservation of tissue cytoarchitecture and most intraretinal connections. Furthermore, various retinal cell markers are still observable in adult human explants after 9 days in culture (Fernandez-Bueno et al., 2012). However, RGC degeneration over prolonged periods has not been investigated in an adult human system.

Understanding ways to model and possibly delay the onset of RGC apoptosis will play an important role in limiting the effects of optic nerve atrophy and aid in the advancement of future regenerative strategies to promote axon regrowth that require the preservation of RGCs after injury.

2 Materials and Methods

2.1 Human explant dissection and culture

Donor human eyes were obtained within 24 hours *post mortem* from the East Anglian Eye Bank or within 2 hours from patients undergoing orbital exenteration under the auspices of the Human Tissue Bank (both facilities within the Norfolk and Norwich University Hospital). All donated material was free of any known retinal pathology and contained no obvious ocular trauma or undiagnosed retinal injury at dissection. Fifty-two *post mortem* donor eyes were used in this study between the age of 30 and 91 years. Unpublished data from a larger cohort of untreated eyes (n=100 donor eyes) was also included for comparative purposes. The four living donor eyes were kindly donated from patients between 59 and 84 years of age. The research was approved by the UK National Research Ethics Committee (REC 04/Q0102/57) and was conducted under the tenets of the Declaration of Helsinki.

Retinal dissection was performed as described previously (Niyadurupola et al., 2011). Briefly, the anterior portion (including the lens and iris) of each donor eye was removed carefully by a circumferential incision at the pars plana (Fig. 1A). A flat retinal preparation was established by removal of the vitreous and cutting small incisions in the peripheral retina (Fig. 1D). The macula removed using a 4mm diameter dissecting trephine (Biomedical Research Instruments, MD, USA) (Fig. 1E) and five para-macular explants, termed human organotypic retinal cultures (HORCs), were dissected from each donor retina using the same trephine. The location of each retinal HORC explant was equidistant from the macula for each donor retina using a template to reduce variability between dissections (Fig. 1G).

4mm circular explants were randomised prior to culture for up to 4 weeks in 35mm culture dishes (Corning, NY, USA) containing 1.5ml of freshly prepared medium. Culture medium included 1) serum free (SF) Dulbecco's Modified Eagle Medium (DMEM)/HamF12, 2) 10% foetal bovine serum (10% FBS) supplemented DMEM/HamF12 or 3) Neurobasal®-A media (NB) with 2% B27 supplement, 1% N2 supplement and 0.8mM L-glutamine (All from Invitrogen, Paisley, UK). All media were supplemented with gentamicin (50 µg/ml; Sigma-Aldrich, Poole, UK) and explants were cultured at 35°C in a humidified atmosphere of 95% air/5% CO_2. Explants were cultured as free-floating preparations, immersed in medium, the RGC side facing upwards. Media was replaced immediately after dissection and half the medium was exchanged twice weekly thereafter.

2.2 Planar retinal sectioning

4mm retinal explants were taken from the macular and para-macular retina of 4 donor eyes, placed RGC side up on filter paper and mounted on a prepared surface of frozen optimal cutting temperature compound (OCT) (Sakura Finetek, Zoeterwoude, Netherlands) as described previously (Niyadurupola et al., 2013). Further OCT was used to cover the sample prior to freezing. 20µm sections in the plane of the retinal nuclear layers were taken using a Bright OTF 5000 cryostat (Bright Instruments, Huntingdon, UK) and individually collected in 1.5ml eppendorfs before being frozen on dry ice.

2.3 Quantitative Real Time PCR (qRT-PCR)

Total RNA was extracted from 221 HORCs using the RNeasy Mini Kit (Qiagen, Crawley, UK) or from 107 planar retinal sections using the RNeasy Micro kit (Qiagen,

Crawley, UK) according to the manufacturer's instructions. The concentration of RNA was measured using a NanoDrop ND-1000 spectrophotometer (NanoDrop Technologies, Wilmington, USA) and reverse transcribed to complementary DNA (cDNA) in a reaction catalysed by Superscript™ II reverse transcriptase with dNTP mix and random primers (all Invitrogen, Paisley, UK).

TaqMan PCR was performed using an ABI Prism 7700 Sequence Detection System (Applied Biosystems, Warrington, UK) using 5ng of input cDNA, Mastermix (Applied Biosystems, Warrington, UK) and probes/primers listed in Table. 1. Whole explant mRNA expression was normalised to the geometric mean of CT values for cytochrome c-1 (*CYC1*) and topoisomerase DNA I (*TOP1*) as described previously (Niyadurupola et al., 2011), whilst planar sections were normalised to the section containing the greatest level of expression. Expression profiles from individual retinas were aligned by matching expression of the photoreceptor marker recoverin (*RCVRN)*.

2.4 Immunohistochemistry and TUNEL analysis

Immunohistochemistry was used to localise and quantify RGC number. 65 explants were fixed in 4% formaldehyde for 24 hours and then cryopreserved in a 30% sucrose solution in PBS at 4°C for a further 24 hours. Explants were embedded in OCT and frozen at -80°C. Transverse 13µm sections were cut via cryostat and mounted on 3'aminopropyl-triethoxyl silane (TESPA, Sigma-Aldrich, Poole, UK) coated glass slides.

Sections were immunostained overnight with RGC markers neuronal nuclei (NeuN) (mouse; 1:250, Millipore, Watford, UK), βIII tubulin (mouse; 1:1000, G7121 Promega,

Southampton, UK or rabbit; 1:1000 MRB-435 Covance, Maidenhead, UK) or Thy-1.1 (mouse; 1:100, Millipore, Watford, UK) diluted in blocking solution (5% goat serum (Invitrogen, Paisley, UK), 0.3% Triton X-100 (Sigma-Aldrich, Poole, UK) in PBS). The DeadEnd™ Fluorometric TUNEL system (TUNEL) (G3250 Promega, Southampton, UK) was performed alongside NeuN immunohistochemistry to visualise apoptotic RGCs as performed previously (Niyadurupola et al., 2011; Osborne et al., 2015). TUNEL staining was carried out the following morning after overnight primary antibody incubation according to manufacturer's instructions. Secondary antibodies of Alexa Fluor 488- and 568–conjugated (Invitrogen, Paisley, UK) (1:1000) were used diluted in blocking solution for 2 hours and nuclei were counterstained with DAPI (1:100; Invitrogen, Paisley, UK).

10 whole-mount explants were fixed in 4% paraformaldehyde for 24 hours followed by 5x PBS washes and blocking (5% goat serum, 0.2% bovine serum albumin (Sigma-Aldrich, Poole, UK), 0.3% Triton X-100 in PBS) for 1 hour. Co-localisation between (NeuN) (1:200 Millipore) and βIII tubulin (1:1000 Covance) was performed via overnight sequential staining using antibodies raised in different species. Following washing and secondary antibody staining, whole-mounts were placed on slides, RGC side up, between two thin plastic parafilm strips (Sigma-Aldrich, Poole, UK) running along either edge of the slide to act as spacers. Samples were then mounted with fluorSave™ reagent (Calbiochem/EMD Chemicals Inc., Gibbstown, NJ, USA) and a coverslip placed on top.

Images were taken using a wide-field Axiovert 200M fluorescence microscope (Zeiss, Welwyn Garden City, UK) or SP5 confocal microscope (Leica Microsystems, Wetzlar,

Germany) at 20 or 40X magnification. Confocal images were obtained via sequential scanning using 0.5µm z-step intervals.

The number of DAPI-labelled nuclei in the RGC layer was quantified using the ImageJ plugin 'Image-based Tool for Counting Nuclei (ITCN)' (http://www.bioimage.ucsb.edu/downloads/automatic-nuclei-counter-plug-in-for-imagej). Software accuracy was >95% comparable to manual counts and any missed nuclei were added using the 'Cell Counter' Plugin. RGC counting and the number of $TUNEL^+$ NeuN labelled cells were assessed manually by a masked investigator from 20 non-overlapping regions per explant. Co-localisation was assessed using Velocity software with an acceptance reading of >0.9 between the two fluorescent dyes. The images shown were from a stack depth of 3µm where clear distinction between individual RGCs could be observed.

2.5 Statistical Analysis

Data shown is the mean ± standard error of the mean (s.e.m). Significance was determined using Student's t-tests or one-way ANOVA with Dunnett's or Tukey's post hoc test (GraphPad Prism; Graph-Pad Software Inc., La Jolla, Ca, USA). Differences were considered significant at the $p \leq 0.05$ level.

3. Results

3.1 RGC marker gene expression in retinal explants

As an indicator of RGC number, the mRNA expression pattern of three commonly used RGC markers (*RBFOX3*, *TUB3* and *THY1*) in human retinal explants (Fig. 2) was investigated. Comparable levels of RGC gene expression were seen in each of the five para-macular explants (no significant differences between explants were observed based on their sampling distribution, *RBFOX3* p=0.8480, *TUB3* p=0.9761, *THY1* p=0.9196, Fig. 2B, C, D). The macula (M), as expected, showed the greatest expression of each marker.

To address concerns relating to donor variability with respect to *post mortem* time, we compared RGC gene expression from *post mortem* samples to that of explants from living donors, when retinal tissue had been obtained as quickly as possible (<2 hours) following orbital exenteration. Results indicated no significant differences in retinal *RBFOX3*, *TUB3* and *THY1* expression between the living donor samples and those excised from *post mortem* tissue (Fig. 2 – red dots).

Further comparisons to assess RGC variations with age were carried out by plotting individual explant gene expression data points against age, which yielded no significant correlation (Fig. 3A, C, E). A similar lack of correlation was observed when comparing *RBFOX3*, *TUB3* and *THY1* to *post mortem* time (Fig. 3B, D, F). Addressing these issues further by comparing *THY1* expression from explants collected from 100 *post mortem* donor eyes revealed the same outcome that neither age (p=0.0911, Fig. 3G) nor *post mortem* time (p=0.8251, Fig. 3H) had any significant influence on RGC expression within the human retina.

3.2 RGC mRNA expression profiling in para-macular and macula explants

To confirm that the investigated RGC markers were expressed in the correct region of the retina, planar sectioning was used. *RBFOX3, TUB3* and *THY1* each showed highest expression in the inner retina for both macular and para-macular explants (Fig. 4). As expected, the macular section yielded of a larger number of sections (approximately 20 compared to 10 at the para-macular locations) due to greater retinal thickness (Fig. 4A). Of the macular sections, a larger number contained RGC mRNA (approximately 8 compared to 4 at the para-macular locations) resulting in a broader peak compared to para-macular regions (Fig. 4B). A similar expression pattern was seen between each of the three RGC markers, which indicated that the markers were likely to be recognising the same cell type.

3.3 Comparison of RGC protein markers in retinal explants

Having shown that *RBFOX3, TUB3* and *THY1* represented useful markers for human RGCs, being differentially expressed across and throughout the retina in their expected locations, we wished to support this data via observation of their protein expression.

NeuN, βIII tubulin and Thy-1 immunohistochemistry in both macular and para-macular human retinal explants supported gene expression data with almost exclusive labelling within the RGC layer (RGCL) (Fig. 5A-C). Using single antibody staining, all $DAPI^+$ cells in the RGC layer were counted and the proportions of these cells that were positive for each RGC marker was quantified. In macular samples, 82.7±1.9% of DAPI stained cells were $NeuN^+$, 80.9±2.6% βIII $Tubulin^+$ and 81.8±1.5% $Thy\text{-}1^+$ (Fig. 5Ai, Bi,

Ci and Table. 2). In para-macular regions, respective RGC markers were 53.7±2.3%, 51.2±0.6% and 52.8±3.3% of all RGCL nuclei (Fig. 5Aii, Bii, Cii and Table. 2). A small number of cells in the INL also stained positive for each antibody indicating likely displaced RGCs or amacrine cells (Fig. 5A-C).

Co-localisation between NeuN and βIII tubulin was then investigated to ensure that the RGC markers were binding to the same cell type within the RGCL. NeuN and βIII tubulin were selected over Thy-1 due to more complete and intense staining of the cell nuclei and soma, which improved evaluation. Both transverse section and whole-mount staining confirmed a strong level of co-localisation between the two markers with approximately 95% of $NeuN^+$ cells staining for βIII $tubulin^+$ (Fig. 6A-D and Table. 3).

3.4 RGC survival with long-term culture

Having shown that NeuN could be used to accurately label RGCs in the human retina, the longevity of RGCs in para-macular retinal explants (HORCs) was assessed over a four-week period. NeuN immunohistochemistry was chosen as the preferred RGC marker to combine with apoptotic labelling due to its discrete staining of the cell body which enabled accurate quantification with the nuclei stain TUNEL. Changes in RGC gene expression were also assessed throughout the four-week period since these may be a more sensitive measure of RGC survival within explants (Niyadurupola et al., 2013). Of the three comparable RGC gene expression markers, we chose to investigate *THY1* to coincide with our previous research modelling short-term RGC degeneration (Niyadurupola et al., 2013; Niyadurupola et al., 2011; Osborne et al., 2015).

Over four weeks in culture, the overall appearance of HORCs showed no obvious structural changes, with explants retaining a considerable degree of histotypic organisation throughout long-term culture (Fig. 7A-E). Outer nuclear, inner nuclear and RGC nuclei were detectable in specific layers throughout the four-week time frame and $NeuN^+$ cells could be detected at all experimental time points.

Quantification of $NeuN^+$ cells at 1 week revealed no significant loss in SF and 10% FBS groups (Fig. 7F) although there was a significant decrease in labelled cells at subsequent time points (23.0±8.3% SF (n=6 donor eyes), 20.8±5.3% 10% FBS (n=3 donor eyes) at week 4, $p \leq 0.05$, Fig. 7F). Greater RGC loss was measured in HORCs cultured in Neurobasal medium (NB) where there was a linear decrease in the number of $NeuN^+$ cells, decreasing approximately 25% (25.2±4.2) at week 1 and by 60% (59.2±7.5) at week 3 ($p \leq 0.05$, n=3 donor eyes, Fig. 7F). Comparisons at 3 and 4 weeks revealed significantly fewer RGCs in explants cultured in NB medium compared to either SF or 10% FBS medium ($p \leq 0.05$, n=3 donor eyes, Fig. 7F).

Assessing the viability of these cells using TUNEL labelling revealed that, although RGCs were detectable, the cells were undergoing time-dependent apoptosis. TUNEL-labelling showed a progressive increase in apoptotic labelling within the RGCL with time for all three treatment groups (Fig. 7G). Under all conditions, there was a significant increase in the number of $TUNEL^+$ NeuN–labelled nuclei at week 1 compared to week 0 ($n \geq 3$ donor eyes/treatment, $p \leq 0.05$, Fig. 7G). $TUNEL^+$ NeuN–labelling continued to increase at weekly intervals with almost all (82.2±7.1 SF, 90.4±0.8 10% FBS, 94.4±2.8 NB) $NeuN^+$ cells staining as apoptotic by week 4 ($p \leq 0.05$,

n≥3 donor eyes/treatment). HORCs taken from a living donor followed a similar trend (Fig. 7G). HORCs cultured in NB medium had the most rapid increase in TUNEL labelling (76.1±11.2) with a significantly higher number of apoptotic RGCs compared to SF (45.0±14.8) and 10% FBS (50.5±12.1) groups at week 1 ($p \leq 0.05$, n=3 donor eyes/treatment).

THY1 gene expression changes supported a decline in RGC viability with time in culture, shown by a rapid decrease in *THY1* immediately after dissection (week 0) to approximately 20% of the post-dissection level after 1 week (SF n=5, 10% FBS n=5, NB n=2 donor eyes, Fig. 7H); expression levels remained at this 20% level for the duration of the experiments. An equivalent relative decline in *THY1* after 1 week was seen in both the retina of the living donor and *post mortem* material. Culturing explants in 10% FBS or NB did not prevent, or accelerate, *THY1* mRNA loss with time compared to SF culture (Fig. 7H).

4. Discussion

Organotypic culture models have become an increasingly popular experimental tool in retinal research, bridging the gap between *in vitro* and *in vivo* experimentation. We were the first to use the human retina to create a quantifiable explant model that can be used to study RGC degeneration (Niyadurupola et al., 2011). In the present study we further characterised markers for human RGCs and showed that *post mortem* human organotypic retinal cultures can be used as a long-term model to study RGC degeneration after axotomy.

4.1 RGC markers in the human retina

Firstly we revealed that neuronal markers for monitoring the RGC population in the rodent eye could be applied to the human retina, with precise and accurate labelling of cell populations within the RGCL. NeuN is widely regarded as being a useful RGC marker (Bull et al., 2011; Canola et al., 2007; Dijk et al., 2007; Zhong et al., 2007) and strong co-labelling has been detected between the antibody and fluorogold retrograde labelled mouse RGCs (Buckingham et al., 2008). Similarly, βIII tubulin has been shown to provide a reliable indicator of the number of surviving RGCs in comparisons with fluorogold-labelled rat RGCs (Cui et al., 2003). Furthermore, whilst Thy-1 transgenic animals have been used frequently in glaucoma research (Raymond et al., 2009). *THY1* mRNA levels have been found by us (Niyadurupola et al., 2011) and others (Nash and Osborne, 1999) to provide a good index of RGC damage.

We initially showed that RGC mRNA expression across the macular and para-macular regions of the retina followed the typical RGC profile for the human retina; with greatest expression in the macula, the central region of the human retina, which is responsible

for the highest visual acuity. The mRNA expression results were in keeping with our previous data, which showed that *RBFOX3 (NeuN)* mRNA decreased from the central macula to the periphery (Niyadurupola et al., 2011). We further demonstrated that, for each of the three RGC markers investigated, the same expression profile was identified and exhibited a consistent organisation throughout the retina; with minimal expression in the outer retina increasing towards maximal expression in the innermost retina where the RGC cell bodies are located.

The mRNA expression data was supported by immunohistochemistry for NeuN, βIII tubulin and Thy-1 that only labelled cells in the inner retina. NeuN staining was located in the cell body (nucleus and surrounding cytoplasm) as has been shown previously (Bull et al., 2011; Raymond et al., 2008) whilst βIII tubulin labelled RGC soma and their processes, similar to the distribution observed in rodent retinas (Johnson and Martin, 2008; Li et al., 2010). Thy-1 is a cell surface glycoprotein that associates with the RGC bodies, dendrites and axons (Nash and Osborne, 1999; Osborne and Larson, 1996; Sheppard et al., 1991) and in our studies labelling was observed primarily on the cell bodies. However labelling was diffuse, probably because Thy-1 is a cell surface marker and resulted, therefore, in Thy-1 being the most challenging to quantify.

Co-localisation of NeuN and βIII tubulin confirmed that either antibody could be used as a reliable marker to quantify RGCs. Others have shown that a co-localisation pattern also exists for Thy-1 and NeuN whereby 95.4% of thy-1-CFP cells in the RGCL also labelled with NeuN (Raymond et al., 2008). In addition, we observed a greater proportion of NeuN, βIII tubulin and Thy-1 positive cells within the RGCL of macular

samples compared to para-macular samples; this would be in keeping with the functional superiority of the central region of the retina with previous estimates suggesting that almost all cells in the RGCL at the human fovea are RGCs (only 3% representing displaced amacrine cells). In para-macular samples the proportion of RGCs in the RGCL decreased to approximately 60%, a similar percentage to that seen in mice and rat retina; whereby approximately 50-60% of cells were RGCs with the remainder being of amacrine origin (Jeon et al., 1998; Perry, 1981). Although we did not measure changes at the periphery, others have shown that the proportion of RGCs can decrease to as few as 20%, with the remainder being of amacrine lineage (Curcio and Allen, 1990). Sampling at the periphery therefore may contain too few RGCs for quantitative neurodegeneration studies.

It should be noted that in rodents βIII tubulin antibodies can cross react with ligands expressed on amacrine cells (Sharma and Netland, 2007). Similarly, probing for NeuN in rats revealed significant INL staining, likely to be that of amacrine cells (Bull et al., 2011; Johnson et al., 2014). However, these latter observations were less apparent in the human retina with very few NeuN or βIII tubulin-labelled cells being identified outside the RGCL. Our results also showed that the proportions of $NeuN^+$ and βIII $tubulin^+$ cells closely matched those that were Thy-1^+ which has been reported by others to exclusively label RGCL cells (Kwong et al., 2010; Liu et al., 2013) or with expression levels several fold higher on RGCs than amacrine cells (Raymond et al., 2009). Furthermore, we believe the appropriateness of these markers can be shown by the differential expression between macular and para-macular regions; It is likely that regional differences would not be seen if labelling was inclusive of amacrine cells. The retinal profiles of *THY1* and the cholinergic amacrine marker *ChAT* also differed

in peak expression indicating a likely difference in cell type detection and that we were accurately measuring just RGC cells (Supplementary Fig. 1).

4.2 The suitability of using *post mortem* human retinal tissue

There has been an assumption that it is not feasible to utilise *post mortem* retina as a model of degeneration due to the extended time from death to retinal isolation. Furthermore, whole-mount retinal analysis has demonstrated previously that RGC number in the human retina can vary considerably between individuals, particular with age (Harman et al., 2000). However, the present results have indicated that RGC mRNA expression (the most sensitive indicator of RGC loss) in the area surrounding the macula does not show a large degree of variability with age or *post mortem* time. Even when eyes were taken with a very short transit time (<2 hours), and from living donors, we did not see a substantial difference in RGC mRNA expression compared to aged, long (up to 24 hours) *post-mortem* time eyes. The rates of *THY1* mRNA loss and apoptotic labelling also revealed little difference between donors. Thus it can be concluded that a rapid degradation of RGC marker mRNA did not occur between death/removal of eyes and dissection. Additionally the degeneration of RGCs from living donors occurred at the same speed implying rate of damage was comparable between tissues.

4.3 Human retinal explants as a model of chronic neurodegeneration

Our final experiments assessed the feasibility of using adult human retina as a long-term culture system for studying RGC degeneration. Of the three RGC markers investigated, NeuN proved quickest, easiest and most reliable to count. Using antibodies to βIII tubulin and Thy-1 led to additional labelling of RGC dendrites and

axons making quantification more time consuming. βIII tubulin and Thy-1 have also proven difficult to assess in rat explants (Bull et al., 2011) and therefore might not be appropriate for large scale analyses. Interestingly, it has been shown that Thy-1 (Huang et al., 2006) and βIII tubulin expression are down regulated following injury, prior to cell loss, which could make NeuN an appropriate RGC marker for immunohistochemical identification and quantification, although the others may be useful therefore in assessing earlier neurodegenerative changes.

As a model of degeneration, retinal explants require complete RGC axotomy, an insult that ultimately leads to RGC death and is associated with *in vivo* models (Levkovitch-Verbin et al., 2013; Wang et al., 2015). The progressive nature of RGC loss, therefore, can provide a useful model in which to investigate the neurodegenerative features of optic nerve degeneration associated with injury or glaucoma.

In our experiments, human explants showed progressive RGC apoptotic labelling with time, with minimal damage immediately post dissection, as observed previously (Niyadurupola et al., 2011), to extensive RGC apoptotic labelling at 4 weeks. The rate of apoptosis closely matched that seen in animal optic nerve crush models (70% of RGCs are apoptotic within the first 14 days after injury (Magharious et al., 2011)), although HORC RGC death appeared to be faster than in rodent explant models (Johnson and Martin, 2008; McKernan et al., 2007). It is unlikely that the species differential effect is due to the extended *post mortem* times seen when using human organotypic cultures because: 1) apoptosis at the beginning of experiments was absent and 2) freshly prepared living donor explants followed a similar rate of cell death to *post mortem* explants. One possibility is that the mediums used did not

contain the necessary growth factors to maintain human RGC survival for such extended times and this warrants further investigation. Support for the assumption that medium composition is important for survival was shown in the experiments where explants displayed variations in the rate of neurodegeneration depending on medium composition.

After we had identified that serum did not improve survival in human explants, we decided to test an alternative SF medium in the hope that this might enhance survival. We opted for the most commonly used medium composition for the survival of RGCs (Bull et al., 2011; Johnson and Martin, 2008) which is also a medium shown to enhance hippocampal neuron survival over 4 weeks in culture (Brewer, 1997); this was Neurobasal®-A with the stated supplements. However to our surprise, we observed a rapid loss of RGCs and increased early apoptosis in the HORCs cultured in Neurobasal medium compared to those in SF DMEM/F12 medium. The reason for the survival differences with the two media was unclear and beyond the scope of this paper, however we can speculate that differences in amino acids, vitamins, ferric nitrate and sodium pyruvate compositions might have played a role, particularly a lack of glutamate and aspartate in NB medium. Additionally, the B27 supplement in NB medium can suppress the growth of glial cells (Brewer et al., 1993), which may dampen the supportive role of these cells in human explants. Identification as to why NB was detrimental to human RGCs would be useful for future investigation although the result does itself highlight that cell soma delivered trophic factors are important in affecting RGC degeneration.

4.4 Further uses of human explants

Although TUNEL labelling was only quantified in the RGC layer, an overall increase in TUNEL labelling could be seen throughout the retina. With apoptosis evident in the INL and ONL, and appearing to increase with time in culture, use of human organotypic cultures may prove useful in the study of other retinal diseases. Rat organotypic cultures, for example, are currently being used to measure growth factor neuroprotection of photoreceptors (Lipinski et al., 2011). Assessing novel neuroprotective strategies relating to retinal neurodegeneration of either photoreceptors (e.g. in age-related macula degeneration or retinitis pigmentosa) or RGCs (e.g. in glaucoma) could be a useful application for this model.

5 Conclusions

Strong similarity between human *post mortem* tissue and living donor retina suggest that human retinal explants could be a valuable resource as a chronic experimental model of RGC degeneration. Various markers can be used to accurately quantify RGC number throughout the retina and alterations to the medium can have an impact on the rate of apoptosis and cell loss. The human explant model therefore provides a platform to investigate future neuroprotective and regenerative therapies, which rely on delaying RGC apoptosis.

Acknowledgements

The authors would like to express their gratitude to all eye donors, Pamela Keeley, Mary Tottman and Samantha Major (of the East Anglian Eye Bank) for donor eye retrieval and both Bridget Hemmant and Marc Moncrief (of the Norfolk and Norwich University Hospital) for providing living donor samples.

References

Albrecht May, C. (2008). Comparative anatomy of the optic nerve head and inner retina in non-primate animal models used for glaucoma research. *Open Ophthalmol J.* **2**, 94-101.

Bobu, C., Lahmam, M., Vuillez, P., Ouarour, A. and Hicks, D. (2008). Photoreceptor organisation and phenotypic characterization in retinas of two diurnal rodent species: potential use as experimental animal models for human vision research. *Vision Res.* **48**, 424-432.

Brewer, G. (1997). Isolation and culture of adult rat hippocampal neurons. *J Neurosci Methods* **71**, 143-155.

Brewer, G. J., Torricelli, J. R., Evege, E. K. and Price, P. J. (1993). Optimized survival of hippocampal neurons in B27-supplemented Neurobasal, a new serum-free medium combination. *J Neurosci Res* **35**, 567-76.

Buckingham, B., Inman, D., Lambert, W., Oglesby, E., Calkins, D., Steele, M., Vetter, M., Marsh-Armstrong, N. and Horner, P. (2008). Progressive ganglion cell degeneration precedes neuronal loss in a mouse model of glaucoma. *J Neurosci.* **28**, 2735-2744.

Bull, N., Johnson, T., Welsapar, G., DeKorver, N., Tomarev, S. and Martin, K. (2011). Use of an adult rat retinal explant model for screening of potential retinal ganglion cell neuroprotective therapies. *Invest Ophthalmol Vis Sci.* **52**, 3309-3320.

Buyens, T., Gaublomme, D., Van Hove, I., De Groef, L. and Moons, L. (2014). Quantitative assessment of neurite outgrowth in mouse retinal explants. *Methods Mol Biol.* **1162**, 57-71.

Caffé, A., Ahuja, P., Holmqvist, B., Azadi, S., Forsell, J., Holmqvist, I., Söderpalm, A. and van Veen, T. (2001). Mouse retina explants after long-term culture in serum free medium. *J Chem Neuroanat.* **22**, 263-273.

Canola, K., Angénieux, B., Tekaya, M., Quiambao, A., Naash, M., Munier, F., Schorderet, D. and Arsenijevic, Y. (2007). Retinal stem cells transplanted into models of late stages of retinitis pigmentosa preferentially adopt a glial or a retinal ganglion cell fate. *Invest Ophthalmol Vis Sci.* **48**, 446-454.

Cui, Q., Yip, H., Zhao, R., So, K. and Harvey, A. (2003). Intraocular elevation of cyclic AMP potentiates ciliary neurotrophic factor-induced regeneration of adult rat retinal ganglion cell axons. *Mol Cell Neurosci.* **22**, 49-61.

Curcio, C. and Allen, K. (1990). Topography of ganglion cells in human retina. *J Comp Neurol.* **300**, 5-25.

Dijk, F., Bergen, A. and Kamphuis, W. (2007). GAP-43 expression is upregulated in retinal ganglion cells after ischemia/reperfusion-induced damage. *Exp Eye Res.* **84**, 858-867.

Donovan, S. and Dyer, M. (2006). Preparation and square wave electroporation of retinal explant cultures. *Nat Protoc.* **1**, 2710-2718.

Engelsberg, K., Ehinger, B. and Ghosh, F. (2008). Early development of retinal subtypes in long-term cultures of human embryonic retina. *Curr Eye Res.* **33**, 185-191.

Fernandez-Bueno, I., Fernández-Sánchez, L., Gayoso, M., García-Gutierrez, M., Pastor, J. and Cuenca, N. (2012). Time course modifications in organotypic culture of human neuroretina. *Exp Eye Res.* **104**, 26-38.

Harman, A., Abrahams, B., Moore, S. and Hoskins, R. (2000). Neuronal density in the human retinal ganglion cell layer from 16-77 years. *Anat Rec.* **260**, 124-131.

Huang, W., Fileta, J., Guo, Y. and Grosskreutz, C. (2006). Downregulation of Thy1 in retinal ganglion cells in experimental glaucoma. *Curr Eye Res.* **31**, 265-271.

Jeon, C., Strettoi, E. and Masland, R. (1998). The major cell populations of the mouse retina. *J Neurosci.* **18**, 8936-8946.

Johnson, E., Doser, T., Cepurna, W., Dyck, J., Jia, L., Guo, Y., Lambert, W. and Morrison, J. (2011). Cell proliferation and interleukin-6-type cytokine signaling are implicated by gene expression responses in early optic nerve head injury in rat glaucoma. *Invest Ophthalmol Vis Sci.* **52**, 504-518.

Johnson, T., Dekorver, N., Levasseur, V., Osborne, A., Tassoni, A., Lorber, B., Heller, J., Villasmil, R., Bull, N., Martin, K. et al. (2014). Identification of retinal ganglion cell neuroprotection conferred by platelet-derived growth factor through analysis of the mesenchymal stem cell secretome. *Brain.* **137**, 503-19.

Johnson, T. and Martin, K. (2008). Development and characterization of an adult retinal explant organotypic tissue culture system as an in vitro intraocular stem cell transplantation model. *Invest Ophthalmol Vis Sci.* **49**, 3503-3512.

Kwong, J., Caprioli, J. and Piri, N. (2010). RNA binding protein with multiple splicing: a new marker for retinal ganglion cells. *Invest Ophthalmol Vis Sci* **51**, 1052-1058.

Levkovitch-Verbin, H. (2004). Animal models of optic nerve diseases. *Eye (Lond).* **18**, 1066-74.

Levkovitch-Verbin, H., Makarovsky, D. and Vander, S. (2013). Comparison between axonal and retinal ganglion cell gene expression in various optic nerve injuries including glaucoma. *Mol Vis.* **19**, 2526-41.

Li, Y., Zheng, H., Liu, P., Chen, Y., She, Z., Xiao, H. and Zhou, G. (2010). The new targets of ouabain in retinal interneurons of Sprague-Dawley rats. *Brain Res Bull.* **81**, 617-624.

Lipinski, D., Singh, M. and MacLaren, R. (2011). Assessment of cone survival in response to CNTF, GDNF, and VEGF165b in a novel ex vivo model of end-stage retinitis pigmentosa. *Invest Ophthalmol Vis Sci.* **52**, 7340-7346.

Liu, B., Sun, X., Suyeoka, G., Garcia, J. and Leiderman, Y. (2013). TGFβ signaling induces expression of Gadd45b in retinal ganglion cells. *Invest Ophthalmol Vis Sci* **54**, 1061-1069.

Magharious, M., D'Onofrio, P., Hollander, A., Zhu, P., Chen, J. and Koeberle, P. (2011). Quantitative iTRAQ analysis of retinal ganglion cell degeneration after optic nerve crush. *J Proteome Res.* **10**, 3344-62.

McKernan, D. P., Guerin, M. B., O'Brien, C. J. and Cotter, T. G. (2007). A Key Role for Calpains in Retinal Ganglion Cell Death. *Invest Ophthalmol Vis Sci.* **48**, 5420-5430.

Nash, M. S. and Osborne, N. N. (1999). Assessment of Thy-1 mRNA levels as an index of retinal ganglion cell damage. *Invest Ophthalmol Vis Sci.* **40**, 1293-8.

Niyadurupola, N., Sidaway, P., Ma, N., Rhodes, J., Broadway, D. and J, S. (2013). P2X7 receptor activation mediates retinal ganglion cell death in a human retina model of ischemic neurodegeneration. *Invest Ophthalmol Vis Sci.* **54**, 2163-2170.

Niyadurupola, N., Sidaway, P., Osborne, A., Broadway, D. and Sanderson, J. (2011). The development of human organotypic retinal cultures (HORCs) to study retinal neurodegeneration. *Br J Ophthalmol.* **95**, 720-726.

Osborne, A., Aldarwesh, A., Rhodes, J., Broadway, D., Everitt, C. and Sanderson, J. (2015). Hydrostatic Pressure Does Not Cause Detectable Changes in Survival of Human Retinal Ganglion Cells. *PLoS One.* **10**, e0115591.

Osborne, N. and Larson, A. (1996). Antigens associated with specific retinal cells are affected by ischaemia caused by raised intraocular pressure: effect of glutamate antagonists. *Neurochem Int.* **29**, 263-70.

Perry, V. (1981). Evidence for an amacrine cell system in the ganglion cell layer of the rat retina. *Neuroscience.* **6**, 931-44.

Raymond, I., Pool, A., Vila, A. and Brecha, N. (2009). A Thy1-CFP DBA/2J mouse line with cyan fluorescent protein expression in retinal ganglion cells. *Vis Neurosci* **26**, 453-465.

Raymond, I., Vila, A., Huynh, U. and Brecha, N. (2008). Cyan fluorescent protein expression in ganglion and amacrine cells in a thy1-CFP transgenic mouse retina. *Mol Vis.* **14**, 1559-1574.

Rojas, C. V., Martínez, J. I., Flores, I., Hoffman, D. R. and Uauy, R. (2003). Gene Expression Analysis in Human Fetal Retinal Explants Treated with Docosahexaenoic Acid. *Invest Ophthalmol Vis Sci.* **44**, 3170-3177.

Sharma, R. and Netland, P. (2007). Early born lineage of retinal neurons express class III beta-tubulin isotype. *Brain Res.* **1176**, 11-7.

Sheppard, A. M., Konopka, M., Robinson, S. R., Morgan, I. G. and Jeffrey, P. L. (1991). Thy-1 antigen is specific to ganglion cells in chicks. *Neurosci Lett* **123**, 87-90.

Wang, X., Lin, J., Arzeno, A., Choi, J., Boccio, J., Frieden, E., Bhargava, A., Maynard, G., Tsai, J. and Strittmatter, S. (2015). Intravitreal delivery of human NgR-Fc decoy protein regenerates axons after optic nerve crush and protects ganglion cells in glaucoma models. *Invest Ophthalmol Vis Sci.* **56**, 1357-66.

Yang, Y., Mao, D., Chen, X., Zhao, L., Tian, Q., Liu, C. and Zhou, B. (2012). Decrease in retinal neuronal cells in streptozotocin-induced diabetic mice. *Mol Vis.* **18**, 1411-1420.

Zhang, X., Li Liu, D., Chiang, S., Choy, K., Pang, C., Lam, D. and Yam, G. (2010). Immunopanning purification and long-term culture of human retinal ganglion cells. *Mol Vis.* **16**, 2867-2872.

Zhong, L., Bradley, J., Schubert, W., Ahmed, E., Adamis, A., Shima, D., Robinson, G. and Ng, Y. (2007). Erythropoietin promotes survival of retinal ganglion cells in DBA/2J glaucoma mice. *Invest Ophthalmol Vis Sci.* **48**, 1212-1218.

Figure captions

Fig. 1: Dissection of the human eye globe to create retinal explants. (A) A circular ring of tissue was removed approximately 10mm below the ciliary body. (B) The eye globe was rotated to dissociate the retina from the underlying retinal pigmented epithelium using the weight of the vitreous to separate the layers. (C) A single cut was performed at the optic nerve head to detach the retina. (D) The vitreous was then removed and the retina spread flat, retinal ganglion cell side up. (E) The macula was removed using a 4mm diameter dissecting trephine. The fovea (white arrow) at the center of the macula could be identified as a shallow depression containing yellow carotenoid pigments lutein and zeaxanthin that indicated accurate macula explant preparation (F). (G) Five 4mm para-macular samples were taken at equidistant locations from the macula using a template to reduce variability between dissections.

Fig. 2: RGC gene expression was comparable between explants taken in the para-macular region with the greatest expression of each marker within macular explants. (A) The dissection template was used to collect all explants and resulted in improved sampling reproducibility. (B) *RBFOX3* (NeuN) mRNA expression in retinal explants (n=11 donor eyes). (C) *TUB3* (βIII tubulin) mRNA expression in explants (n=11 donor eyes). (D) *THY1* mRNA expression in explants (n=15 donor eyes). All mRNA was normalised to the expression of the housekeeping genes *TOP1* and *CYC1*. Graphs show individual values for each explant including the mean ± s.e.m. Explants A-E are taken within the para-macular region of the retina, M are samples dissected at the macular. Red data points highlight explants taken from 2 living donor eyes.

Fig. 3: RGC gene expression was not significantly influenced by the age of the donor or the time between donor death and retinal explant creation (*post mortem* time). (A-F) Each data point represents a single para-macular explant and indicated that there was no significant correlation between the expression of *RBFOX3* (n=49 explants), *TUB3* (n=49 explants) or *THY1* (n=68 explants) with parameters that could influence RGC starting number. (G, H) *THY1* expression from a larger cohort of untreated eyes (n=100 donor eyes) taken immediately after dissection similarly revealed no correlation between donor age, *post mortem* time and gene expression. All mRNA was normalised to the expression of the housekeeping genes *TOP1* and *CYC1*.

Fig. 4: Gene profiling revealed the location of RGC markers *RBFOX3*, *TUB3* and *THY1* throughout the retina in macular (A) and para-macular (B) explants. Up to 21x 20µm sections were collected throughout the entire retinal thickness and processed in the plane of the retinal nuclear layers from the photoreceptor layer (left) to the retinal ganglion cell (RGC) layer (right). A greater number of sections were collected from macular explants due to the highest thickness in this region, with a broader RGC peak due to a denser, thicker RGC layer. Similar expression patterns were seen between *RBFOX3*, *TUB3* and *THY1* in both macular and para-macular regions. (*RBFOX3* n=3 donor eyes (for both macular and para-macular explants), *TUB3* n=4 donor eyes, *THY1* n=3 donor eyes; mean ± s.e.m).

Fig. 5: Retinal ganglion cell (RGC) markers NeuN, βIII tubulin and Thy-1 labelled nuclei almost exclusively in the RGC layer of macular and para-macular explants (A-C). Para-macular explants contained a single row of RGCs that stained positive for each marker whilst macular samples had a denser RGC layer with multiple rows of

NeuN, βIII tubulin and Thy-1 labelled cells. NeuN staining was located in the cell body (nucleus and surrounding cytoplasm), βIII tubulin labelled RGC soma and their processes and Thy-1 resulted in diffuse cell body staining. Scale = 50μm (n=4 donor eyes).

Fig. 6: Co-localisation of NeuN and βIII tubulin in transverse (A, C) and whole-mount (B, D) sections revealed both markers were specifically labelling the same cell type in the RGC layer. Similar levels of co-localisation could be seen in macular and para-macular regions of the retina. Scale = 50μm (n=5 donor eyes).

Fig. 7: The survival of human retinal ganglion cells (RGCs) in *ex vivo* para-macular explants (HORCs) over 4 weeks. Representative immunofluorescence photomicrographs of HORCs cultured in SF medium at (A) 0 weeks post dissection, (B) 1 week, (C) 2 week, (D) 3 week, (E) 4 week. (F) The percentage of $NeuN^+$ cells in the RGC layer (mean ± s.e.m; n=3-6 donor eyes) relative to same donor counts immediately post dissection. (G) The proportion of $TUNEL^+$ $NeuN^+$ cells in the RGC layer (mean ± s.e.m; n=3-6 donor eyes) with time in culture. (H) The change in *THY1* mRNA expression (mean ± s.e.m; n=2-6 donor eyes) with time in culture relative to same donor expression immediately after explant creation. DAPI = blue, NeuN = green, TUNEL = red. White arrows highlight $TUNEL^+$ $NeuN^+$ cells in the RGC layer. GCL = ganglion cell layer, INL = inner nuclear layer, ONL = outer nuclear layer. Red data points = Living donor explants cultured in SF medium. Scale = 50μm. *, †, ‡ indicates a statistically significant differences compared to samples processed immediately after dissection in SF, 10% FBS and Neurobasal (NB) medium

respectively. § indicates a significant difference between SF and NB results at the same time point.

Table. 1: List of TaqMan probe/primer sets used in the experiments.

Table. 2: The percentage of DAPI positive cells that stained positive for individual RGC markers in the RGCL (n=4 donor eyes).

Table. 3: The percentage of NeuN labelled cells that were also βIII tubulin positive in macular and para-macular explants (n=5 donor eyes).

Supplementary Fig. 1: Gene profiling of the RGC marker *THY1* (A) and the cholinergic amacrine marker *ChAT* (B) throughout macula explants revealed differences in the location of maximal gene expression. *THY1* peaked in the inner retina whereas *ChAT* expression was detected at greatest levels within the inner nuclear layer (n=3 donor eyes; mean ± s.e.m).

Table. 1

Gene	Number/Sequence	Supplier
RBFOX3	Hs01370653_m1	Applied Biosystems, Warrington, UK
TUB3	Hs00801390_s1	Applied Biosystems, Warrington, UK
THY1	Hs00174816_m1	Applied Biosystems, Warrington, UK
TOP1	HK-DD-hu-300	Primer Design, Southampton, UK
CYC1	HK-DD-hu-300	Primer Design, Southampton, UK

Table. 2

A

	NeuN	βIII tubulin	Thy-1
Macular	82.7±1.9%	80.9±2.6%	81.8±1.5%
Para-macular	53.7±2.3%	51.2±0.6%	52.8±3.3%

B

	Co-localisation between NeuN and βIII tubulin
Macular	95.0±2.3%
Para-macular	93.4±3.0%

Competing interests

No competing interests declared.

Author contribution

A.O. conceived this study. A.O. M.H. and J.S. designed the experiments. A.O., M.H. and P.W. performed the experiments. A.O., M.H. and P.W. analysed the data. A.O. and J.S. interpreted the data being published. The manuscript was written by A.O. and edited by J.S. and D.C.B.

Funding

The Edith Murphy Foundation, The International Glaucoma Association, The Norwich Glaucoma Research Fund, AstraZeneca, University of East Anglia, Faculty of Science and The Humane Research Trust.

1 HUMAN RETINAL DISSECTION

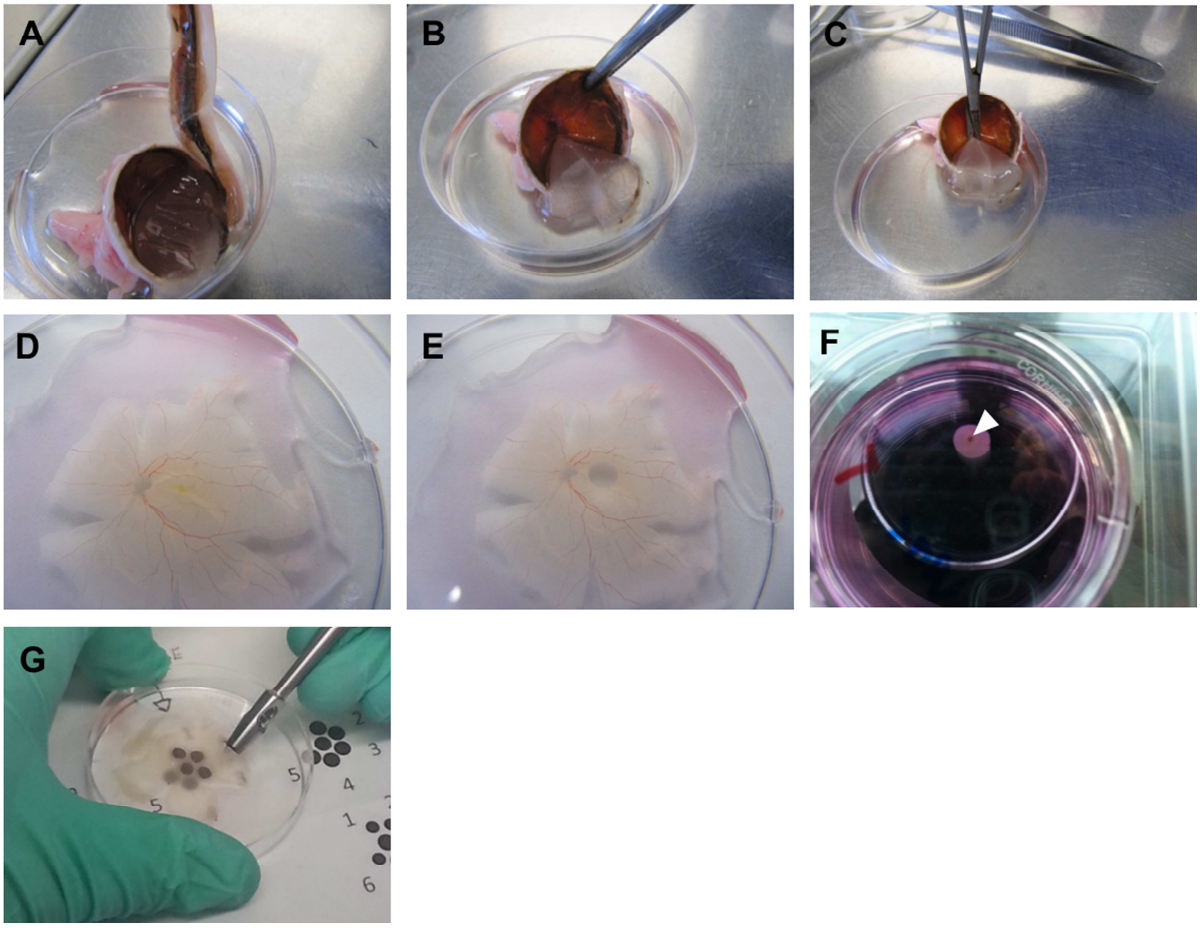

2 EXPLANT RGC GENE EXPRESSION

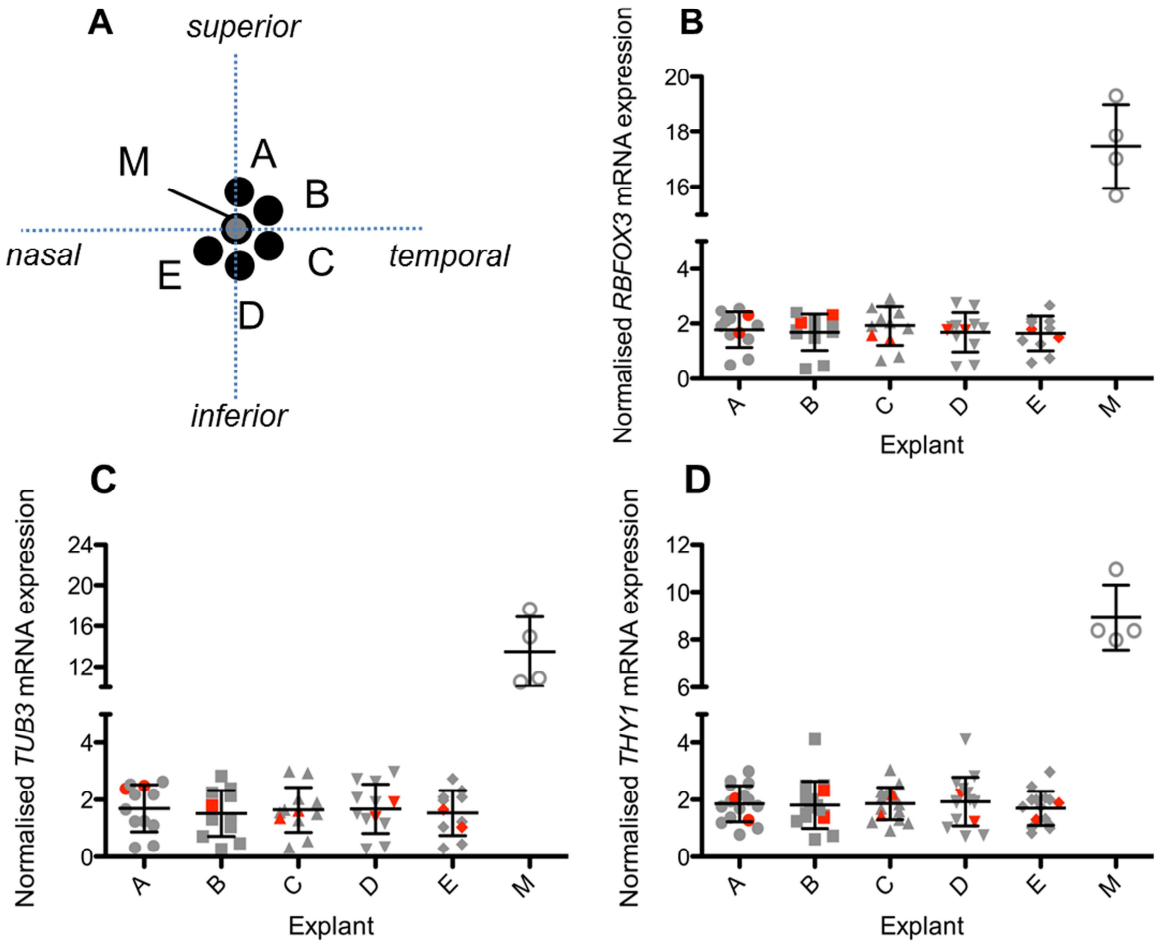

3 CORRELATION OF RGC GENE EXPRESSION

AGE

POST MORTEM TIME

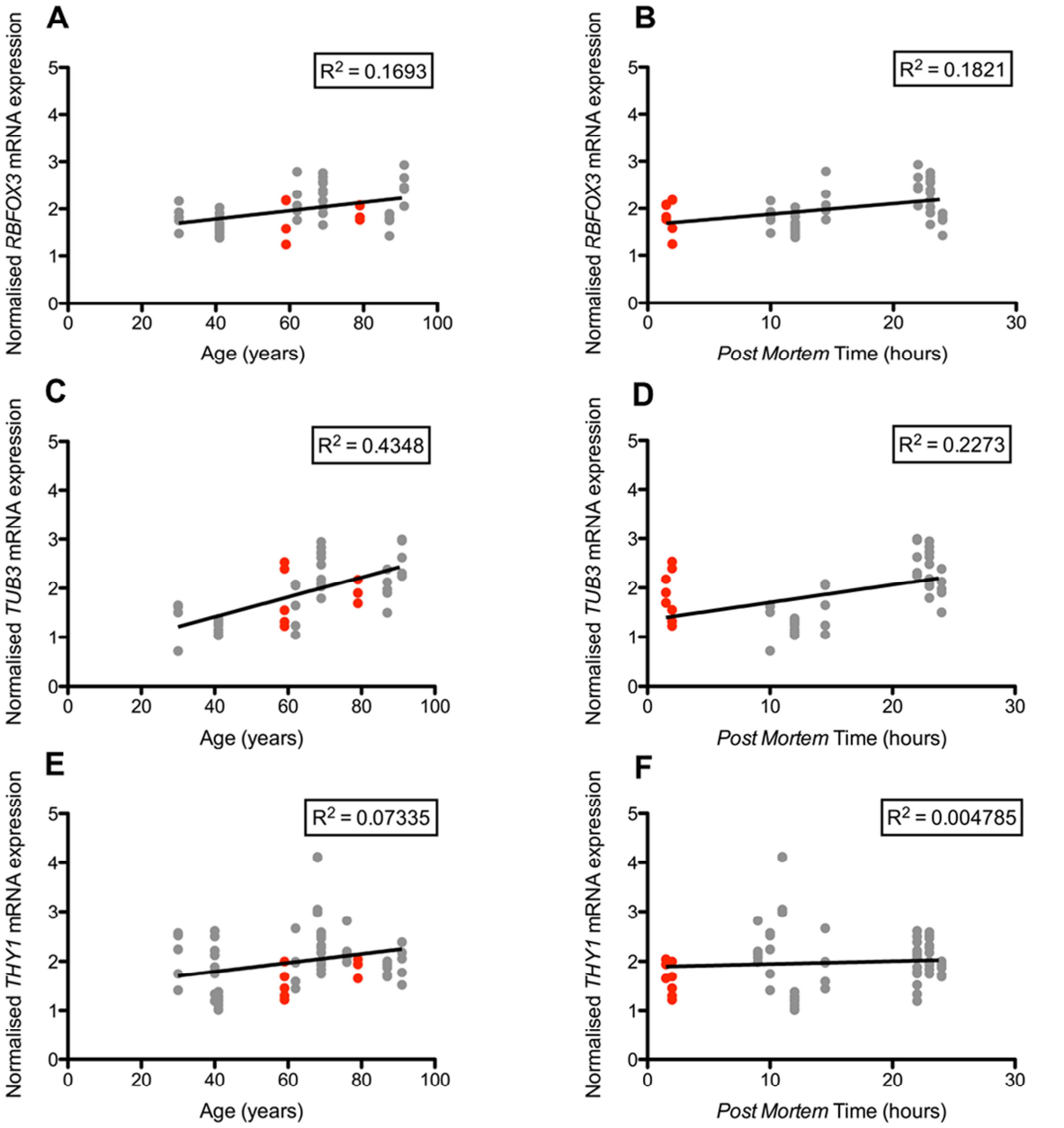

THY-1 EXPRESSION FROM OVER 100 DONOR EYES

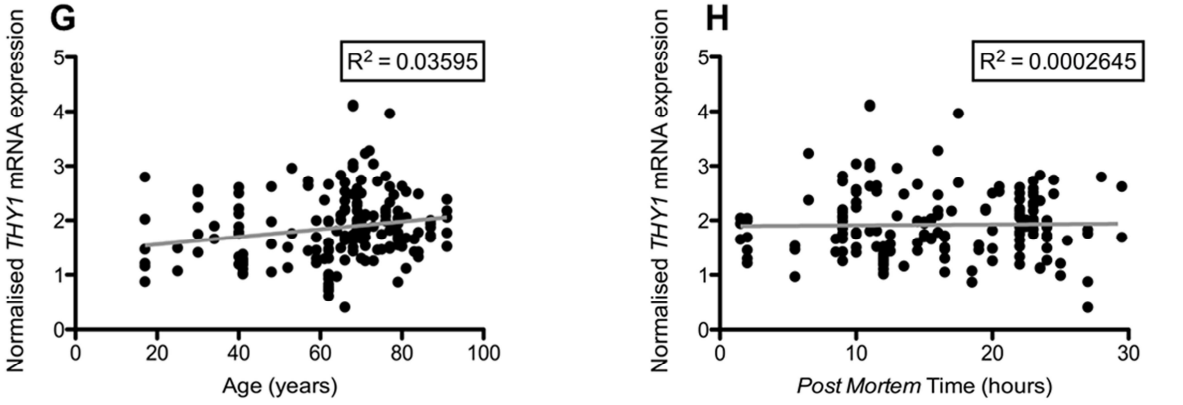

4 PLANAR RETINAL SECTIONS

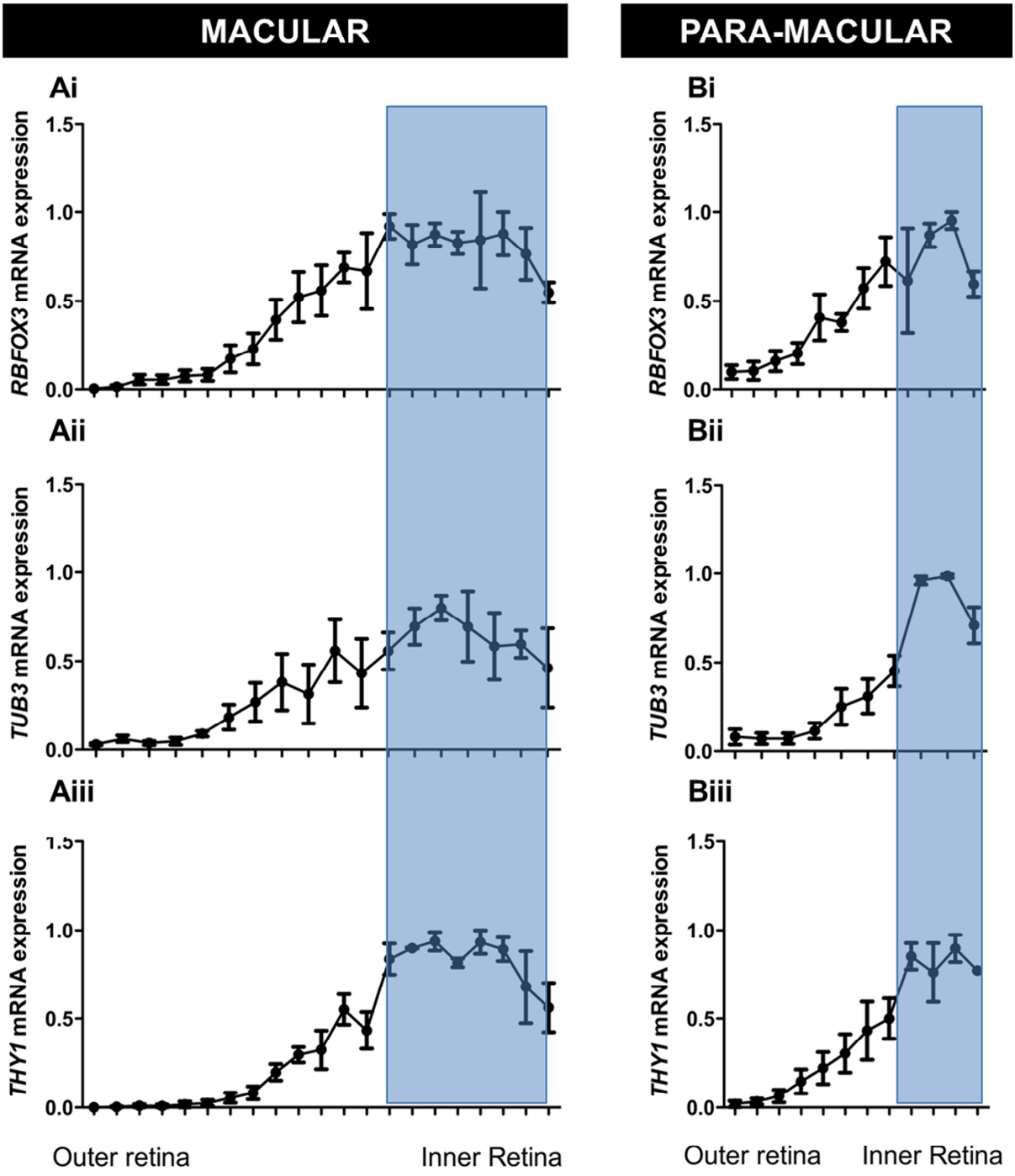

5 TRANVERSE SECTIONS

Macular

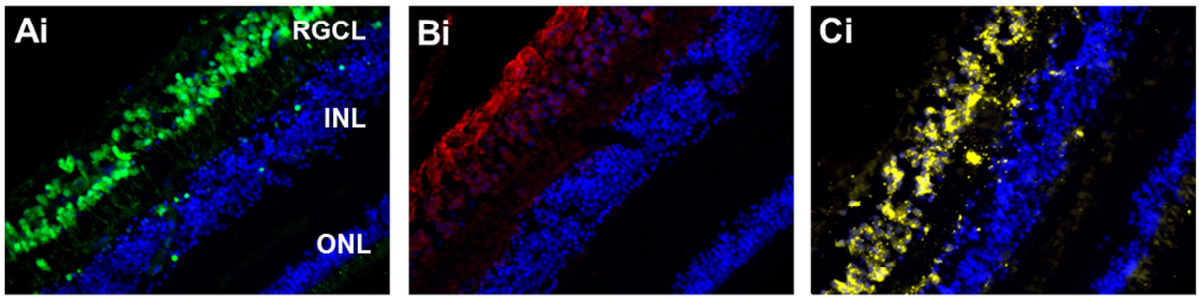

Para-macular

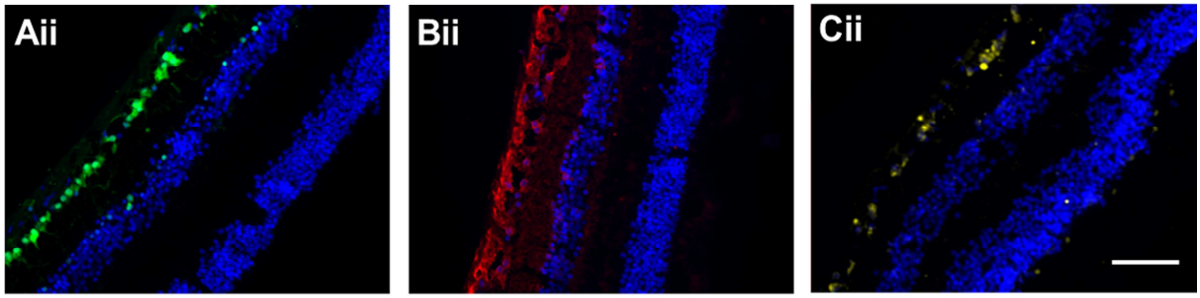

NeuN βIII Tubulin Thy-1

6 TRANVERSE SECTIONS

WHOLEMOUNT SECTIONS

Macular

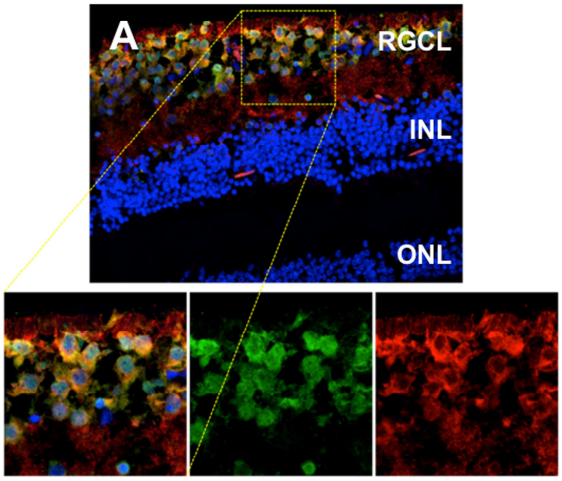

Composite NeuN βIII Tubulin

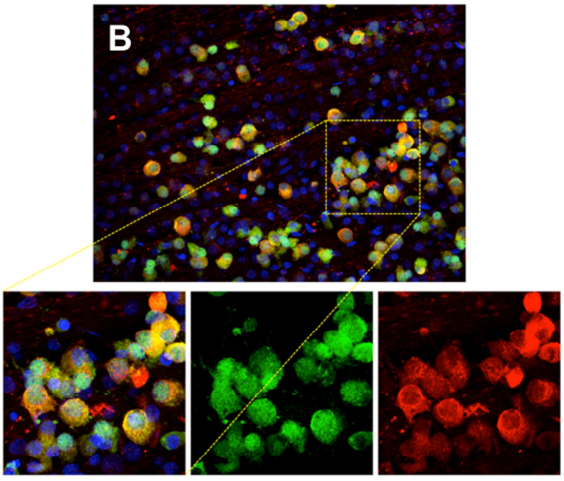

Composite NeuN βIII Tubulin

Para-macular

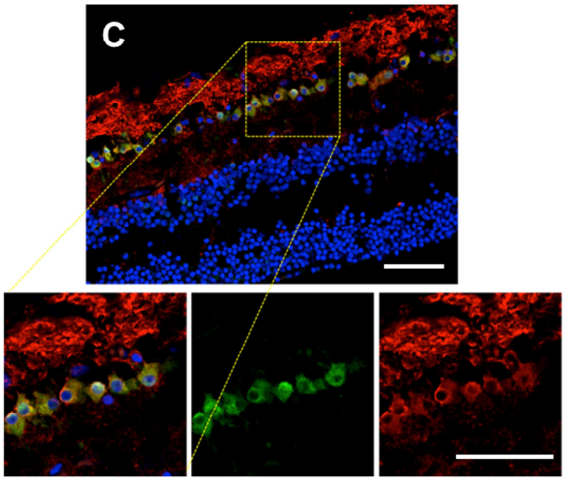

Composite NeuN βIII Tubulin

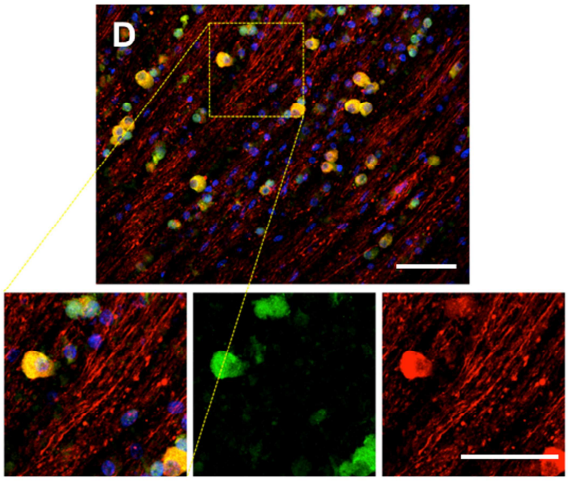

Composite NeuN βIII Tubulin

7 LONG-TERM HUMAN RGC SURVIVAL

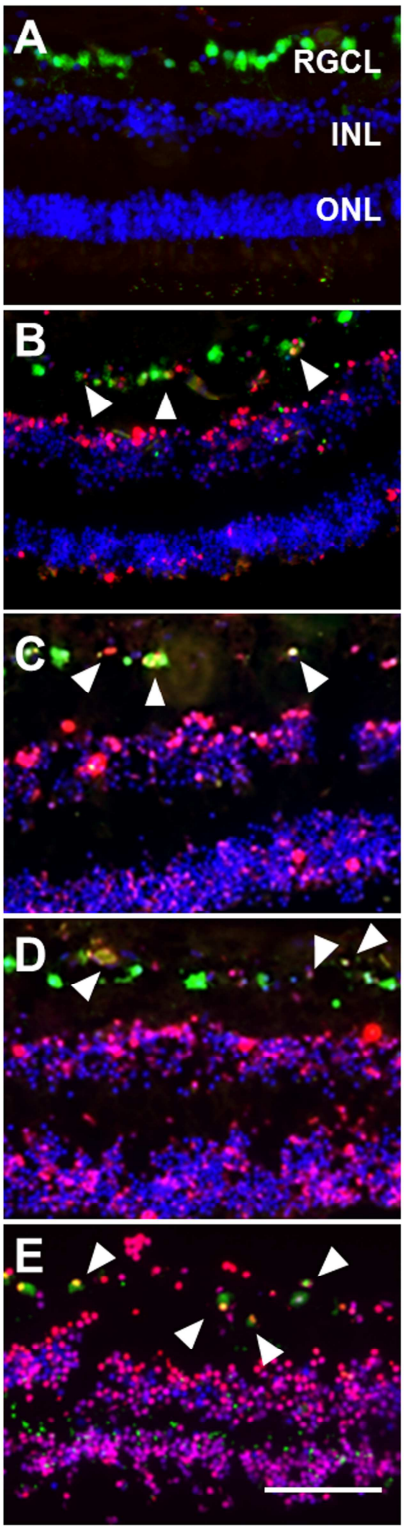

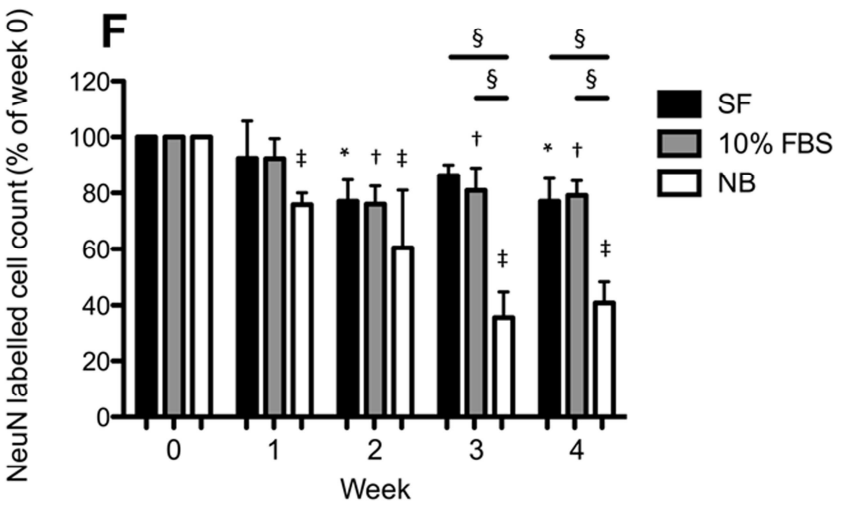

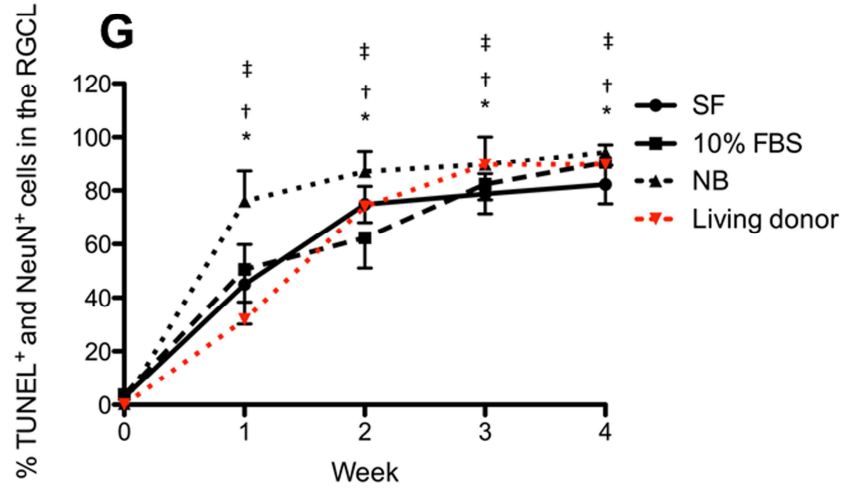

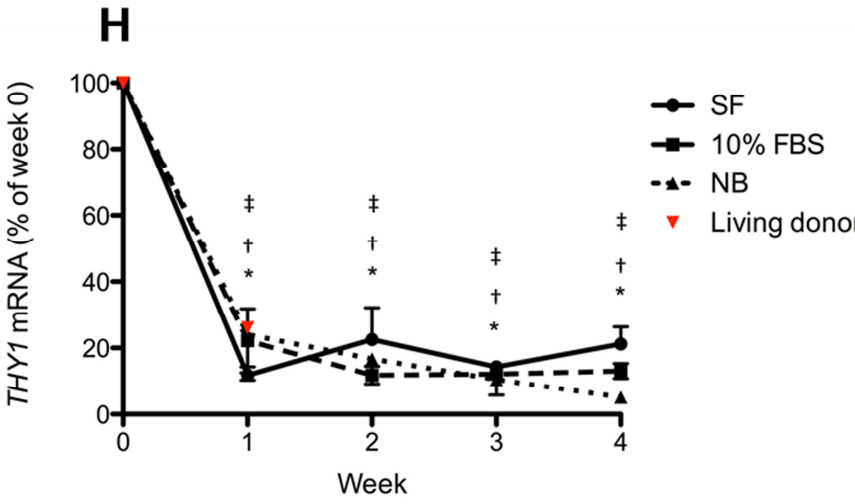

S1 PLANAR MACULAR RETINAL SECTIONS